



Palladium (II) complexes with the unsymmetrical H-spirophosphorane ligand HP(OCMe₂CMe₂O)(OCH₂CMe₂NH): Synthesis, structural and catalytic studies

Anna Skarżyńska*, Andrzej Gniewek

Faculty of Chemistry, University of Wrocław, ul. F. Joliot-Curie 14, 50-383 Wrocław, Poland

ARTICLE INFO

Article history:

Received 10 February 2011

Received in revised form

27 April 2011

Accepted 13 May 2011

Keywords:

Hydrophosphoranes

Palladium

C–C bond formation

Heck reaction

Hiyama reaction

ABSTRACT

We have investigated the reactivity of the unsymmetrical H-spirophosphorane (HSP) ligand HP(OCMe₂CMe₂O)(OCH₂CMe₂NH) **1** towards different palladium(II) precursors and synthesised the mononuclear complexes [PdCl₂{P(OCMe₂CMe₂O)OCH₂CMe₂NH₂}] **2** and [PdCl(C₃H₅){P(OCMe₂CMe₂O)OCH₂CMe₂NH₂}] **3**. The structural features of the compounds are characterised by spectroscopic methods as well as single crystal X-ray diffraction studies. The complexes are shown to be remarkably active precatalysts for the Heck and Hiyama cross-coupling reactions. The products of the C–C bond formation reactions were obtained with high conversion and stereoselectivity. Mechanistic studies of the Heck reaction reveal that, besides homogenous precatalysts, also heterogeneous Pd(0) nanoparticles are involved in the catalytic process.

© 2011 Elsevier B.V. All rights reserved.

1. Introduction

Heterofunctionalised, bidentate P,E ligands (E = N, O) constitute an important, widely utilised group of ligands in transition metal chemistry. The vast majority of these compounds comprise heteroditopic phosphines, where the phosphorus is the soft donor, and the hard donor is either a nitrogen or oxygen atom. Less attention has been paid to mixed bidentate phosphites. Albeit phosphite ligands in particular P,N heterodonors, have demonstrated to be an effective ligands for asymmetric catalytic reactions such as allylic alkylation and Heck cross-coupling reactions [1]. Therefore we believe that construction of new mixed P,N ligands that can be easily synthesised from starting material is of great importance. For this purpose H-spirophosphoranes, capable of P,N- or P,O-coordination seem to be particularly useful because of their easy designing. Recently palladium complexes incorporating H-spirophosphorane (HSP) ligands have emerged as efficient catalyst precursors for Heck cross-coupling reactions [2]. The reported results show that the H-spirophosphorane palladium complex [PdCl(μ-Cl){P(OCMe₂CMe₂O)OCMe₂CMe₂OH}]₂ has proved to be a very good catalyst for the reaction of aryl bromide with *n*-butyl acrylate, while the complex [PdCl₂{P(OCH₂CMe₂NH)OCH₂CMe₂NH₂}] shows high activity in the cross-coupling of aryl bromide

not only with *n*-butyl acrylate but also with substituted styrenes. Moreover, the catalyst turns out to be highly effective in the Hiyama coupling reaction of functionalised styrylsilanes with bromobenzene [3]. The outstanding features of H-spirophosphoranes, such as facile synthetic accessibility [4,5] and ambidentate electronic properties (π -acceptor ability of the phosphorus atom along with σ -donor ability of the nitrogen atom), make them attractive for the construction of new palladium precursors suitable for catalytic processes [6]. Given our interest in the coordination abilities of H-spirophosphoranes, we were curious to investigate how fine-tuning inside the ligand molecule could influence catalytic activity.

As a part of our continuing research on the chemistry of H-spirophosphorane ligands, we report on the syntheses of unsymmetrical spirophosphorane palladium complexes, an exploration of their reactivity and application as precatalysts in the Heck and Hiyama coupling reactions.

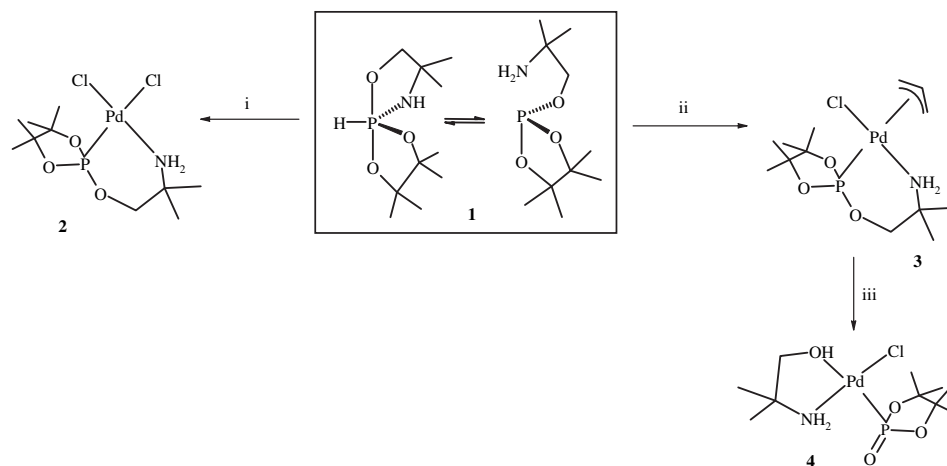
2. Results and discussion

2.1. Synthesis and spectroscopic characterisation

The unsymmetrical H-spirophosphorane ligand HP(OCMe₂CMe₂O)(OCH₂CMe₂NH) **1** was prepared by one-pot synthesis in two stages (eqs. (1) and (2)). It was obtained from equimolar amounts of pinacol and 2-amino-2-methyl-1-propanol in the presence of one equivalent of hexamethylphosphorous triamide P(NMe₂)₃. Pinacol

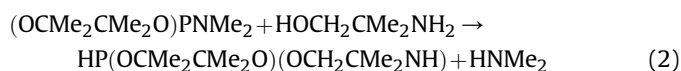
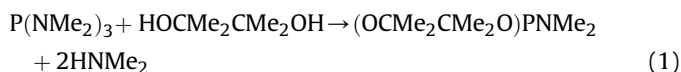
* Corresponding author. Tel.: +48 713757254.

E-mail address: zag@wchuw.r.pl (A. Skarżyńska).



Scheme 1. (i) $[\text{PdCl}_2(\text{cod})]$, dichloromethane; (ii) $[\text{Pd}(\text{m-Cl})(\text{C}_3\text{H}_5)_2]$, toluene; (iii) dichloromethane, $+\text{H}_2\text{O}$, $-\text{C}_3\text{H}_6$.

was the precursor of choice for the first stage, which proceeded smoothly to give $(\text{OCMe}_2\text{CMe}_2\text{O})\text{PNMe}_2$, whereas the use of aminoalcohol in the second step prevented the undesirable symmetrical product $\text{HP}(\text{OCH}_2\text{CMe}_2\text{NH})_2$ from arising in the system. Although some spectroscopic data for **1** are already known (^{31}P NMR [7], there has been no information about the molecular and crystal structure determination. Therefore, we present the stereochemistry of **1** and, additionally, a detailed instrumental analysis.



The $^{31}\text{P}\{^1\text{H}\}$ NMR spectrum of **1** at room temperature exhibits two resonances, at $\delta = -49.21$ ppm and $\delta = 148.45$ ppm, due to the presence of two tautomeric penta- and tri-coordinated forms of phosphorus atom. The presence of a P–H bond was manifested not only in the ^{31}P NMR spectrum but also in ^1H NMR as a doublet at 7.49 ppm with $^1J(\text{P-H}) = 772.5$ Hz. Besides the resonances assigned to the proton at the phosphorus atom, the ^1H NMR spectrum exhibited signals for the NH proton: a doublet at $\delta = 2.78$ ppm, and signals assigned to CH_2 protons: two multiplets at $\delta = 3.54$ ppm and $\delta = 3.57$ ppm assigned to equatorial and axial protons. Additionally, six singlets were detected in the aliphatic resonance range, attributed to six unequal methyl protons. The presence of P–H and N–H

groups found reflection in infrared spectra. Absorption bands for appropriate stretching frequencies are present at $\nu(\text{P-H}) = 2362$ cm^{-1} and $\nu(\text{N-H}) = 3350$ cm^{-1} respectively.

Complexation reactions of ligand **1** were carried out with the use of two palladium precursors: $[\text{PdCl}_2(\text{cod})]$ (cod = 1,5-cyclooctadiene) and $[\text{Pd}(\mu\text{-Cl})(\text{C}_3\text{H}_5)_2]$ (Scheme 1). An equimolar reaction of **1** with appropriate precursors gave rise to the mononuclear chelating complexes $[\text{PdCl}_2\{\text{P}(\text{OCMe}_2\text{CMe}_2\text{O})\text{OCH}_2\text{CMe}_2\text{NH}_2\}]$ **2** (i) and $[\text{PdCl}(\text{C}_3\text{H}_5)\{\text{P}(\text{OCMe}_2\text{CMe}_2\text{O})\text{OCH}_2\text{CMe}_2\text{NH}_2\}]$ **3** (ii) respectively. Ligand **1** coordinates in its predictable tautomeric form, via tricoordinated phosphorus and nitrogen atoms. Both complexes were isolated as yellow or white solids, well soluble in dichloromethane and acetonitrile. Prolonged exposure of dichloromethane solution of **3** to atmospheric moisture causes a new palladium(II) complex, $[\text{PdCl}\{\text{P}(\text{O})(\text{OCMe}_2\text{CMe}_2\text{O})\}\text{HOCH}_2\text{CMe}_2\text{NH}_2]$ **4**, to form as yellow crystals suitable for X-ray structural analysis (see Supplementary material). It is apparently formed as a result of hydrolytic cleavage of a coordinated H-spirophosphorane ligand and simultaneous loss of the allyl molecule. The presence of released propene was confirmed by means of GC–MS in an experiment performed in a tube sealed with a rubber tap. The H-spirophosphorane ligand underwent hydrolytic rupture to form 2-amino-2-methyl-propanol-1 bounded to palladium in a protonated N,O chelating mode and the phosphonate moiety $\text{P}(\text{O})(\text{OCMe}_2\text{CMe}_2\text{O})$ coordinated via the phosphorus atom.

The chemical compositions of **2** and **3** were ascertained by microanalytical and spectroscopic data. ^1H NMR spectra for both complexes at room temperature show first-order patterns with

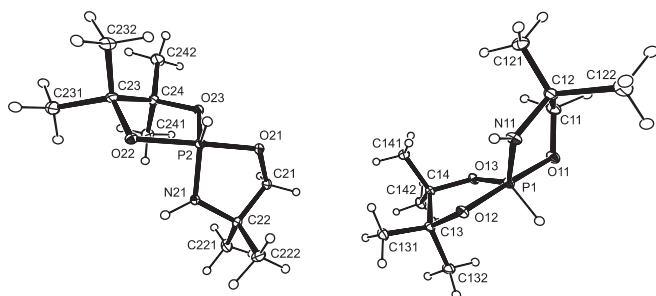


Fig. 1. Molecular structure of ligand **1**. Displacement ellipsoids are drawn at the 30% probability level and H atoms are shown as small spheres of arbitrary radii.

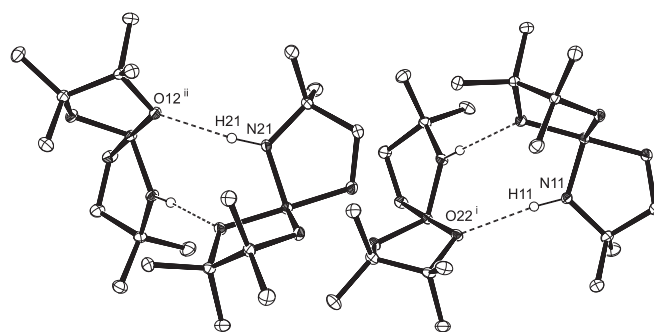


Fig. 2. Hydrogen bonds in ligand **1**. Hydrogen atoms not involved in hydrogen interactions are omitted for clarity. Symmetry codes: (i) $0.5 + x, y, 0.5 - z$; (ii) $-0.5 + x, y, 0.5 - z$.

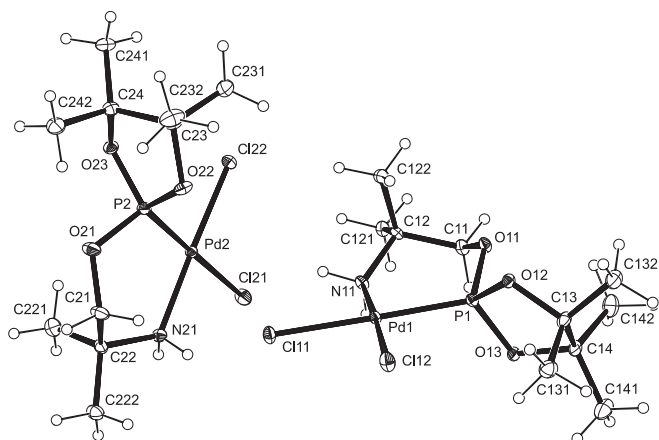


Fig. 3. Molecular structure of complex **2**. Displacement ellipsoids are drawn at the 30% probability level and H atoms are shown as small spheres of arbitrary radii.

three singlets in the range from 1.26 to 1.58 ppm, relevant to six magnetically unequal methyl protons, as well as a doublets at 4.01 and 3.95 ppm, (for **2** and **3**) assignable to CH₂ protons. The presence of wide singlets at 3.93 and 5.01 ppm for both **2** and **3** respectively corresponds to the NH₂ fragment of coordinated H-spirophosphorane ligands. Furthermore, the appearance of NH₂ groups is also supported by characteristic vibrations of IR spectra: $\nu(\text{NH}_2) = 3126\text{--}3239\text{ cm}^{-1}$, which is in accordance with the literature data published for similar moieties [8]. Complexation of the ligand, remarkably seen in the IR spectrum (lack of $\nu(\text{P}\text{--}\text{H})$ stretching vibration), is also manifested in ³¹P{¹H} NMR analysis. The spectra of **2** and **3** exhibit resonances at 90.70 and 134.85 ppm respectively.

2.2. X-ray structural determination

Single crystal X-ray diffraction analyses reveal that the stereochemistry of ligand **1** and complex **2** are nearly identical as those expected from the spectroscopic studies. The molecular structures of **1** and **2** are shown in Figs. 1 and 3 respectively. Details of the structural determination as well as a list of selected bond lengths

Table 1

Crystal data for HP(OCMe₂CMe₂O)(OCH₂CMe₂NH) **1** and [PdCl₂{P(OCMe₂CMe₂O)OCH₂CMe₂NH₂}] **2**.

	1	2
Empirical formula	C ₁₀ H ₂₂ NO ₃ P	C ₁₀ H ₂₂ Cl ₂ NO ₃ PPd
Formula weight	235.26	412.56
Temperature (K)	100(2)	100(2)
λ (Å)	0.71073	0.71073
Crystal system	Orthorhombic	Orthorhombic
Space group	<i>Pbca</i>	<i>Pbcn</i>
<i>a</i> (Å)	14.744(3)	14.056(4)
<i>b</i> (Å)	18.658(4)	16.508(4)
<i>c</i> (Å)	18.807(4)	27.388(6)
Volume (Å ³)	5174(2)	6355(3)
<i>Z</i>	16	16
<i>D</i> _{calc} (g cm ⁻³)	1.208	1.725
μ (mm ⁻¹)	0.20	1.60
<i>F</i> (000)	2048	3328
Crystal size (mm)	0.58 × 0.40 × 0.12	0.25 × 0.12 × 0.10
θ range(°)	3.0–27.5	3.0–27.5
Number of collected reflection	53841	49696
Independent reflection (<i>R</i> _{int})	5939	7301
<i>S</i>	1.02	0.87
<i>R</i> ₁ / <i>wR</i> ₂ indices	0.033/0.091	0.031/0.064

$$R_1 = \frac{\sum ||F_o| - |F_c||}{\sum |F_o|}$$

$$wR_2 = \frac{\{\sum [w(F_o^2 - F_c^2)^2]\}}{\{\sum [w(F_o^2)^2]\}}^{1/2}$$

$$w = 1/[\sigma^2(F_o^2) + (aP)^2] \text{ where } P = (F_o^2 + 2F_c^2)/3, a = 0.0602 \text{ (1), } 0.0316 \text{ (2).}$$

Table 2

Relevant bond distances (Å) and angles (°) for HP(OCMe₂CMe₂O)(OCH₂CMe₂NH) **1**.

Bond lengths			
P1–O11	1.6866(9)	P2–O21	1.6819(9)
P1–O12	1.7146(9)	P2–O22	1.7144(9)
P1–O13	1.6177(9)	P2–O23	1.6198(9)
P1–N11	1.638(2)	P2–N21	1.639(2)
Bond angles			
O13–P1–O11	91.15(5)	O23–P2–O21	91.41(5)
O13–P1–O12	90.72(4)	O23–P2–O22	90.94(4)
O13–P1–N11	122.64(5)	O23–P2–N21	123.11(5)
O11–P1–O12	177.78(5)	O21–P2–O22	177.59(4)
N11–P1–O11	89.67(5)	N21–P2–O21	89.78(5)
N11–P1–O12	90.34(5)	N21–P2–O22	89.38(5)

Table 3

Hydrogen bond geometry (Å, °) in ligand **1**.

D–H...A	D–H	H...A	D...A	D–H...A
N11–H11...O22 ⁱ	0.88	2.15	3.030 (2)	173
N21–H21...O12 ⁱⁱ	0.88	2.15	3.002 (2)	162

Symmetry codes: (i) 0.5 + x, y, 0.5 – z; (ii) –0.5 + x, y, 0.5 – z.

and bond angles are given in Tables 1, 2 and 4. The structures of **1** and **2** are comprised of two crystallographically independent molecules in an asymmetric unit.

The coordination environment of the phosphorus atoms in the free ligand HP(OCMe₂CMe₂O)(OCH₂CMe₂NH) molecule is, as anticipated, a distorted trigonal bipyramid (TBP), with two oxygen atoms, O1n and O2n (*n* = 1, 2), in apical positions. The third oxygen atom, O3n (*n* = 1, 2), the nitrogen atom as well as hydrogen occupy equatorial positions. The angles O11–P1–N11, O13–P1–O12, O21–P2–N21 and O22–P2–O23 around phosphorus atoms are almost 90°. Noticeable distortion from the ideal angle of 120° is observed for the angles O3n–Pn–Nn1 (*n* = 1, 2), which are widened to 122.64(5) and 123.11(5)° respectively. The axial distances Pn–O3n (*n* = 1 or 2), 1.6177(9) Å and 1.6198(9) Å, as stated for the related compounds, are shorter than the two other equatorial distances, P1–O1n and P2–O2n (*n* = 1 or 2) (Table 2) [9]. In the crystal lattice, two adjacent molecules are alternately stabilised by intermolecular hydrogen bonds N–H...O (Fig. 2, Table 3). The presence of such bonds has also been determined for analogous symmetrical phosphorus compounds, e.g. HP(OCH₂CH₂NH)₂, HP(OC₆H₄NH)₂, HP(OCOCHRNH)₂ R = CH₃, C₃H₇ [10–12].

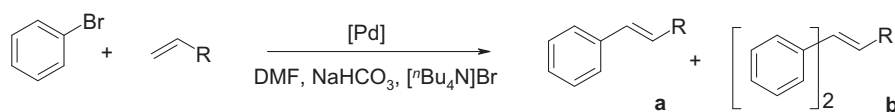
The molecules of **2** are specified by phosphorus and nitrogen atoms of the chelating H-spirophosphorane ligand and two chlorides in *cis* positions. The coordination sphere of the palladium atom in [PdCl₂{P(OCMe₂CMe₂O)OCH₂CMe₂NH₂}] is close to square planar. The phosphorus atoms, Pn (*n* = 1, 2), subtly deviate from the plane defined by the Nn1, Cln1, Cln2, (*n* = 1, 2) atoms by 0.089 and

Table 4

Relevant bond distances (Å) and angles (°) for [PdCl₂{P(OCMe₂CMe₂O)OCH₂CMe₂NH₂}] **2**.

Bond lengths			
Pd1–Cl11	2.3810(9)	Pd1–P1	2.1888(9)
Pd1–Cl12	2.2866(9)	Pd2–P2	2.195(2)
Pd2–Cl21	2.365(2)	Pd1–N11	2.070(3)
Pd2–Cl22	2.2805(9)	Pd2–N21	2.068(3)
Bond angles			
Cl12–Pd1–Cl11	92.98(3)	N11–Pd1–P1	93.07(8)
Cl22–Pd2–Cl21	91.99(4)	N21–Pd2–P2	95.06(8)
P1–Pd1–Cl12	88.87(4)	N11–Pd1–Cl12	176.95(7)
P2–Pd2–Cl22	87.65(4)	N21–Pd2–Cl22	177.28(8)
P1–Pd1–Cl11	178.15(3)	N11–Pd1–Cl11	85.08(8)
P2–Pd2–Cl21	178.47(3)	N21–Pd2–Cl21	85.29(8)

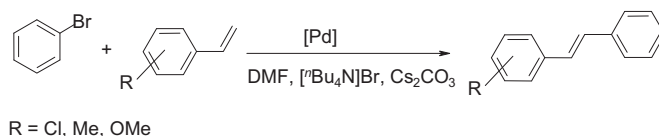
Table 5
Product distribution in the Heck coupling reactions of bromobenzene and butyl acrylate catalysed by the palladium complexes **2** and **3**.



R	Catalyst 2		Catalyst 3	
	Yield % of (a)	Yield % of (b)	Yield % of (a)	Yield % of (b)
C(O)OBu	70	30	72	28

[Pd-complex] $1.35 \cdot 10^{-5}$ mol; NaHCO₃ $4.4 \cdot 10^{-3}$ mol; [tBu₄N]Br $2.3 \cdot 10^{-3}$ mol; PhBr ($4.36 \cdot 10^{-3}$ mol); CH₂=CHC(O)OBu $1.9 \cdot 10^{-3}$ mol; 140 °C, 4 h; mesitylene as internal standard.

Table 6
Product distribution in the Heck coupling reactions of bromobenzene and substituted styrenes catalysed by complexes **2** and **3**.



Entry	RC ₆ H ₄ CH=CH ₂	Catalyst 2		Catalyst 3	
		Conversion of PhBr (%)	Yield (%) of <i>trans</i> -stilbene	Conversion of PhBr (%)	Yield (%) of <i>trans</i> -stilbene
1	3-MeC ₆ H ₄ CH=CH ₂	77	74	91	88
2	4-MeC ₆ H ₄ CH=CH ₂	69	66	83	81
3	2-ClC ₆ H ₄ CH=CH ₂	68	64	82	81
4	4-ClC ₆ H ₄ CH=CH ₂	91	88	98	94
5	4-OMeC ₆ H ₄ CH=CH ₂	69	66	99	95

[Pd-complex] $1.35 \cdot 10^{-5}$ mol; base Cs₂CO₃ $4.4 \cdot 10^{-3}$ mol; [tBu₄N]Br $2.3 \cdot 10^{-3}$ mol; PhBr $1.89 \cdot 10^{-3}$ mol; RC₆H₄CH=CH₂ $2.12 \cdot 10^{-3}$ mol; 140 °C; 4 h; mesitylene as internal standard.

0.051 Å respectively. More remarkable deviations from the ideal square planar values, 90 and 180°, are exhibited by the bond angles at the metal centre (see Table 4). The six-membered metal chelate cycles are fixed to half-chair conformations, while the five-membered phosphorus cycles exhibit envelope conformations. The nature of the donor atoms: phosphorus or nitrogen, seems to have a profound effect on the Pd–Cl bonds. The Pd–Cl₁ bond lengths of 2.3810(9) and 2.365(2) Å are slightly longer than those of Pd–Cl₂, 2.2866(9) and 2.2805(9) Å ($n = 1, 2$), due to a greater *trans* influence of the phosphorus atom with respect to the nitrogen

atom. The Pd–N₁ bond lengths of 2.070(3) and 2.068(3) Å are similar to those found for complexes of the formula PdCl₂(P ~ N), as they are associated with sp³-hybridised amino nitrogen atoms [13–15]. Other bonding parameters in **2** do not differ significantly from the expected values reported for the related complexes.

2.3. Catalytic application of complexes **2** and **3**

As previously outlined, palladium(II) complexes incorporating hydrospirophosphorane ligands appeared to be excellent

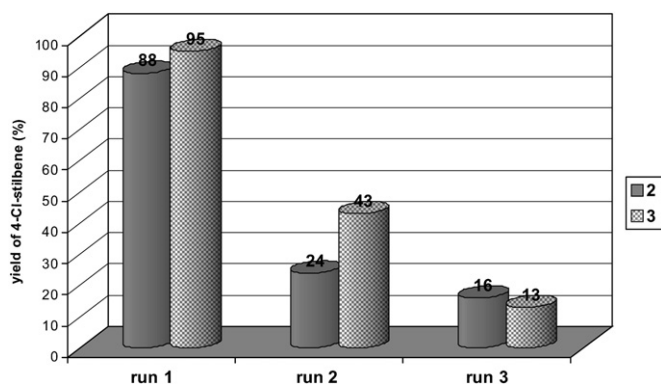


Fig. 4. Catalyst recycling for the Heck coupling of bromobenzene with 4-Cl-styrene and the catalyst precursors [PdCl₂{P(OCMe₂CMe₂O)OCH₂CMe₂NH₂}] **2** and [PdCl(C₃H₅){P(OCMe₂CMe₂O)OCMe₂CMe₂NH₂}] **3**.

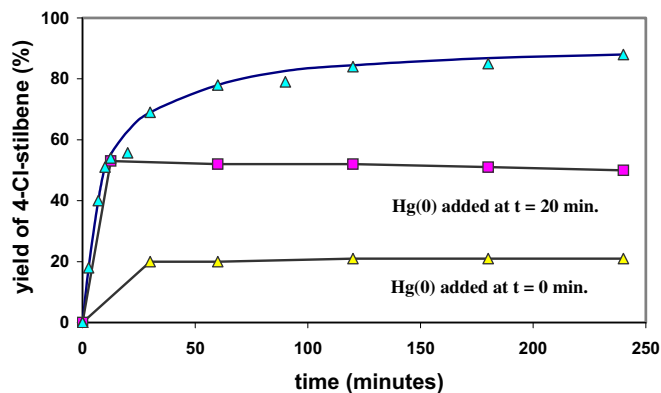


Fig. 5. Reaction profile study of the Heck cross-coupling of 4-Cl-styrene and bromobenzene using **2** as a precatalyst (reaction conditions as stated above) and a poisoning tests with Hg(0) as an inhibitor.

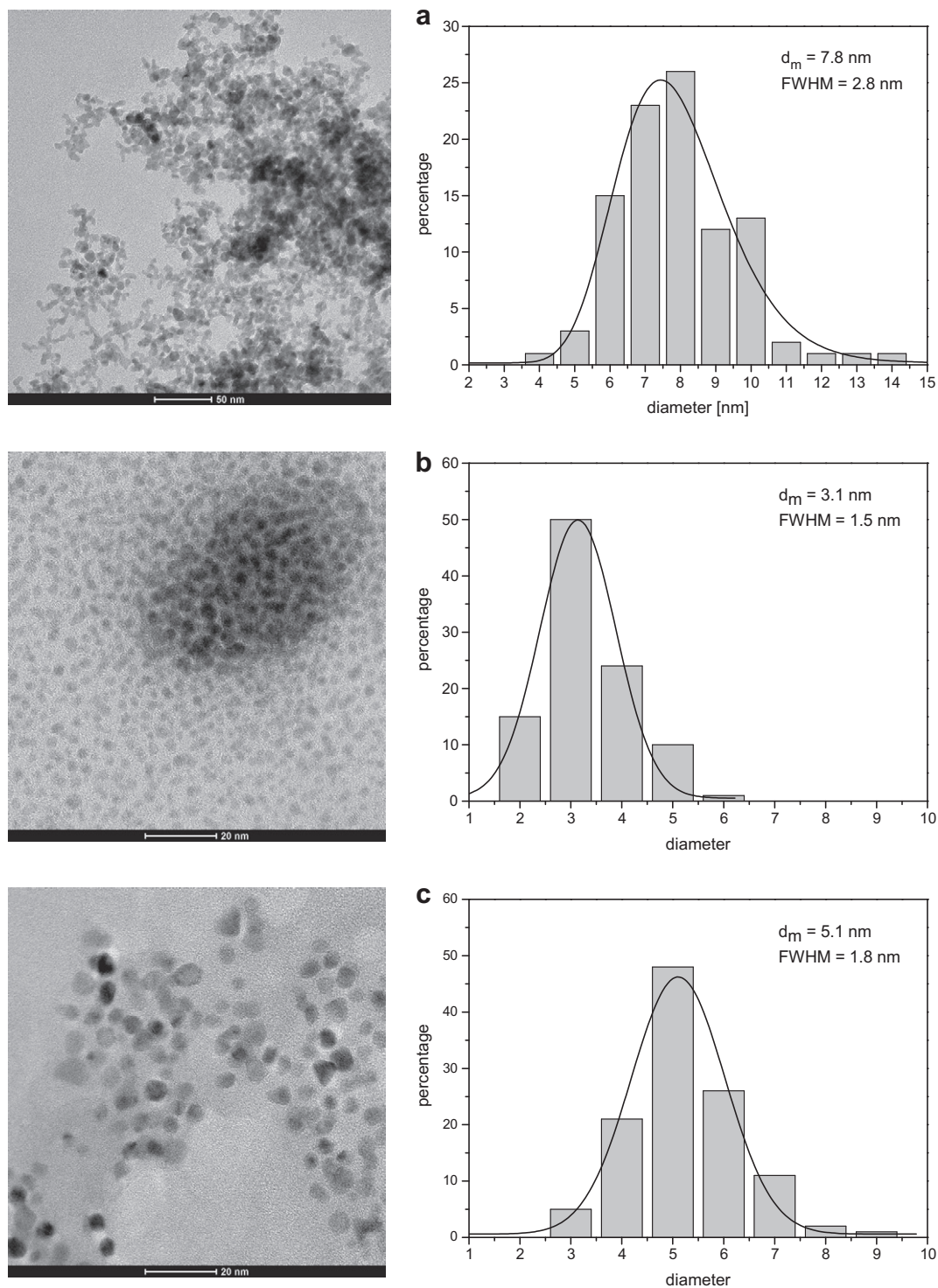
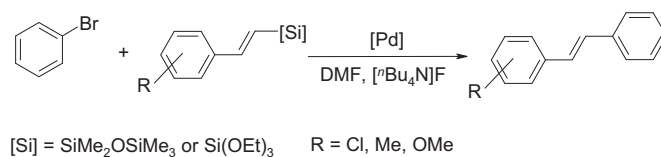


Fig. 6. TEM images and corresponding size histograms (100 nanoparticles measured) of (a) post-catalytic solution using complex **2** as the precatalyst (b) nanoparticles [**Pd2**] synthesised from complex **2** under hydrogen atmosphere in THF (c) post-catalytic solution using [**Pd2**] as a precatalyst.

precatalysts for the Heck and Hiyama cross-coupling reactions [2,3]. This observation directed our interest to the catalytic properties of complexes **2** and **3**. The methodology of the Heck process was utilised as optimised before. The coupling reactions were efficiently performed at an elevated temperature of 140 °C, over a relatively short reaction time of 4 h, in the presence of the polar aprotic solvent DMF, which remains the favoured medium for the

Heck reaction. Since a positive effect of an ionic liquid has been reported in the literature, [ⁿNBu₄]Br was used as an additive, leading to remarkable rate enhancements. Different terminal alkenes, *n*-butyl acrylate and substituted styrenes, were chosen as substrates for the development of the bromobenzene coupling. The obtained results showed that both H-spirophosphorane complexes, **2** and **3**, are very active in the Heck cross-coupling. As seen from

Table 7
Product distribution in the Hiyama coupling reactions of bromobenzene and substituted styrylsilanes catalysed by complexes **2** and **3**.



Entry	RC ₆ H ₄ CH=CH[Si]	Catalyst 2		Catalyst 3	
		Conversion of PhBr (%)	Yield (%) of <i>trans</i> -stilbene	Conversion of PhBr (%)	Yield (%) of <i>trans</i> -stilbene
1	3-MeC ₆ H ₄ CH=CHSi(OEt) ₃	98	96	98	96
2	4-MeC ₆ H ₄ CH=CHSiMe ₂ OSiMe ₃	99	98	99	97
3	2-ClC ₆ H ₄ CH=CHSiMe ₂ OSiMe ₃	99	93	97	91
4	4-ClC ₆ H ₄ CH=CHSiMe ₂ OSiMe ₃	100	97	100	98
5	4-OMeC ₆ H ₄ CH=CHSiMe ₂ OSiMe ₃	98	97	99	96

[Pd-complex] 1.35 · 10⁻⁵ mol; PhBr 1.31 × 10⁻³ mol, ArCH = CH[Si] 1.44 × 10⁻³ mol; activator [nBu₄N]F 2.14 · 10⁻³ mol; 140 °C; 4 h; mesitylene as internal standard.

Table 5, the arylation of *n*-butyl acrylate performed in the presence of NaHCO₃, in the case of both **2** and **3**, proceeds smoothly with 100% conversion to produce mainly a monosubstituted product, i.e. butyl cinnamate **a**, in comparable amounts for both precatalysts.

We found Cs₂CO₃ to be a superior base over NaHCO₃ for the reaction of bromobenzene and substituted styrenes as coupling partners. The relevant results showing a high degree of selectivity are presented in Table 6. Incorporation of an allyl group into the molecule of **3** instead of one chloride ligand had a beneficial effect. [PdCl(C₃H₅){P(OCMe₂CMe₂O)OCH₂CMe₂NH₂}] was found to be a more effective precatalyst compared to **2**, for which lower yields of *trans*-stilbenes were produced. The reaction tolerates a variety of functionalities. The best effects for precatalyst **3** were obtained for a styrene bearing both electron-withdrawing and electron-donating substituents in a *para* position, 4-ClC₆H₄ and 4-OMeC₆H₄ respectively (entry 4 and 5).

Recycling experiments were carried out in reactions of bromobenzene and 4-chlorostyrene (Fig. 4). They were conducted using two methods: extraction of organic products with ethyl ether and loading a new portion of substrates, [nBu₄N]Br, and the base Cs₂CO₃ or filtration of solid components and product extraction from the liquid phase. Similar results were obtained in both cases: after the first run, the catalyst activity degraded and the yield decreased noticeably. This finding (as stated below) might suggest either the aggregation of nanoparticles formed *in situ* in the system or the metal leaching from the NPs.

To get a better understanding of the mechanism of the reaction, we made an attempt to define the nature of the true active species. A variety of experiments or tests have been used to determine the essence of the active species in palladium catalysed reactions [16]. There is no single clear-cut experiment to distinguish between homogeneous catalysts and heterogeneous ones. Therefore, we carried out some mechanistic studies. The reaction profile curve of product yield against time (Fig. 5) indicates that the process starts immediately, and over 50% yield of the appropriate stilbene is achieved within 20 min. The lack of an induction period as well as sigmoidal kinetics, characteristic of heterogeneous catalysts formed *in situ* from monometallic precatalysts, point to the contribution of homogeneous catalyst. However, the induction interval may be too short to be detected in some cases for heterogeneous catalysis. The widely used test to identify the nature of the catalyst is the poisoning mercury test, however it is not universally applicable [16c,17]. The inhibition of catalysis by Hg(0), which amalgamates the metal catalyst or adsorbs on its

surface, is evidence of heterogeneous catalysis [16c] as well as the presence of Pd(0) species in the system [16b]. In our case, the addition of an excess of mercury (260 equivalents) before the reaction and after 20 min (at this time the yield is 54%) causes the suppression of catalytic activity (Fig. 5). This outcome shows that, besides homogeneous species, also Pd(0) species might be involved in this catalytic process. Actually, both the formation of a dark reaction solution and the presence of small Pd(0) nanoparticles observed in TEM micrographs in the post-catalysis liquid phase (Fig. 6a) confirmed this conjecture. The mean particle diameter and size distribution were calculated by counting 100 particles from the enlarged micrographs. The size distribution plot was fitted by means of a log-normal curve approximation. The obtained nanoparticle size distribution is practically symmetric with a well-defined maximum at 7.8 nm and a relatively narrow FWHM of 2.8 nm. Most of the Pd(0) particles are round-shaped; however, some of them form quite irregular aggregates. The nanoparticles obtained *in situ* during the Heck reaction from complex **2** might be additionally stabilised with phosphorous ligands. Energy dispersive X-ray microanalysis (EDX) showed that the Pd:P ratio is about 20:1 in the case of the particles presented in Fig. 6a. To further explore the nature of the phosphorus moieties, complex **2** and other Heck reaction components in a 1:10 ratio were placed in an NMR tube. The ³¹P NMR spectra were recorded in deuterated DMF at an elevated temperature (373 K) for 2 h. During that time only one signal was observed at δ = 10.61 ppm, which might suggest the formation of a new non-innocent phosphorous ligand involved in the catalytic process. In order to understand the effect of the formation of PdNPs on catalytic activity we have synthesised nanoparticles [Pd₂] starting from complex [PdCl₂{P(OCMe₂CMe₂O)OCH₂CMe₂NH₂}] **2** under a hydrogen atmosphere in THF (1 atm, r.t., 56 h) adopting the procedure previously described [17b]. The transmission electron microscopy analysis of [Pd₂] shows the presence of regularly dispersed NPs of spherical shape with an average size of 3.1 nm, exhibiting the tendency to partial organisation (Fig. 6b). [Pd₂] was efficiently used as a catalytic precursor in cross-coupling reaction between bromobenzene and 4-Cl-styrene (140 °C, 4 h, 2.5 mol% Pd) to give 4-Cl-stilbene in 86% yield. The TEM analysis of post-catalytic solution (Fig. 6c) reveals that the NPs remained still dispersed but the mean size increases to 5.1 nm. Performed experiments might suggest involvement of PdNPs in catalytic process which could serve as a reservoir of soluble Pd(0) active species [18].

The catalytic activity of the complexes **2** and **3** was compared in the Hiyama coupling of bromobenzene and functionalised styrylsilanes. Like in the Heck procedure, the experiments were performed under aerobic conditions at 140 °C in DMF over 4 h, but [¹⁸Bu₄N]F was employed as an activator. The presence of both electron-withdrawing and electron-donating groups was tolerated in the coupling under these conditions. The reaction gave almost exclusively substituted *trans*-stilbenes with excellent yields exceeding 96%, except when an electron-withdrawing substituent was present in the *ortho* position in an aromatic ring (Table 7, entry 3).

3. Conclusions

The unsymmetrical H-spirophosphorane ligand HP(OCMe₂CMe₂O)(OCH₂CMe₂NH) **1**, readily obtained from reaction of hexamethylphosphoramide with 2-amino-2-methyl-propanol-1 and pinacol, leads to palladium(II) mononuclear complexes with a chelating P,N coordination mode. In contrast to the stable complex [PdCl₂{P(OCMe₂CMe₂O)OCH₂CMe₂NH₂}] **2**, the allyl analogue [PdCl(C₃H₅){P(OCMe₂CMe₂O)OCH₂CMe₂NH₂}] **3** undergoes hydrolytic cleavage connected with the rupture of coordinated spirophosphorane and the formation of the phosphonate compound [PdCl{P(O)(OCMe₂CMe₂O)}HOCH₂CMe₂NH₂}] **4**. The catalytic potential of complexes **2** and **3** was tested in C–C coupling reactions. The presented results show that under similar reaction conditions the complexes are relatively high-yielding and stereoselective catalysts for Heck and Hiyama cross-couplings. Very small disparity was observed in catalytic performance on changing from unhindered to sterically hindered styrenes or styrylsilanes utilised as substrates. Little effect was also noticed when using electron-withdrawing or electron-donating substrates. Finally, differences in the yield of *trans*-stilbenes observed in the Heck coupling imply to some extent that subtle changes of the pre-catalyst structure may influence the reaction progress. The mechanistic investigations indicate that, besides homogenous precatalysts, Pd(0) nanoparticles formed *in situ* in the system might also be involved in the catalytic process.

4. Experimental section

4.1. General procedure

Chemicals and deuterated solvents were purchased from Sigma–Aldrich and Fluka and used as received. All preparations were performed in an atmosphere of dry, oxygen-free nitrogen, using conventional Schlenk techniques. Solvents were carefully dried and deoxygenated by standard methods [19]. [PdCl₂(cod)] and [Pd(μ-Cl)(C₃H₅)₂] were synthesised as previously reported [20,21].

IR and FIR measurements were performed in KBr or Nujol with a Bruker 113V FTIR. ¹H, ³¹P{¹H} NMR spectra were obtained on Bruker Avance 500 MHz spectrometer (500 MHz for ¹H NMR). The chemical shifts (δ) are given in ppm towards TMS (¹H) and H₃PO₄ (³¹P) using deuterated solvents as lock and reference (¹H) respectively. Elemental analyses were performed on a 2400 CHNS Vario EL III apparatus. Analytical gas chromatographic (GC) analyses were performed on a Hewlett Packard 5890. Conversion of the substrates was calculated using the internal standard method. MS spectra were measured on an ESI Finnigan Mat TSQ 700 instrument. TEM measurements were carried out using a FEI Tecnai G² 20 X-TWIN electron microscope (TEM) operating at 200 kV. Specimens for TEM studies were prepared by putting a droplet of a suspension on a copper microscope grid covered with a perforated carbon film.

4.2. Synthesis of the ligand HP(OCMe₂CMe₂O)(OCH₂CMe₂NH) **1**

The ligand precursor HP(OCMe₂CMe₂O)(OCH₂CMe₂NH) 2,2,3,3,8,8-hexamethyl-1,4,6-trioxo-9-aza-5λ⁵-phosphaspiro[4.4]nonane **1** was obtained using the general procedure described in the literature [22,7]. A mixture of P(NMe₂)₃ (4.36 cm³, 24 mmol) and pinacol (Me₂COH)₂ (2.81 g, 24 mmol) was placed in a round-bottomed flask equipped with a magnetic stirrer and a reflux condenser and heated gradually to 140 °C over 3 h with gentle nitrogen purging. The progress of the reaction was monitored by GC–MS analyses. The lack of pinacol in the system indicated the end of the first stage, and next 2-amino-2-methyl-1-propanol (2.29 cm³, 24 mmol) was added to the cooled mixture. Further stirring with purging over 2 h at 140 °C led to a final white solid. The crude product was purified by recrystallisation from hexane in a freezer providing crystals suitable for X-ray analysis. Yield: 2.5 g (44%).

Anal. Calc. for C₁₀H₂₂NO₃P: C, 51.05; H, 9.43; N, 5.95 Found: C, 50.82; H, 9.78; N, 5.84%; ¹H NMR (C₆D₆) δ 0.95, 0.98, 1.14, 1.15, 1.16, 1.25 (18H, s, s, CH₃), 2.78 (1H, d, ²J(P, H) = 17.5 Hz, NH), 3.54 (1H, q, ²J(H_a, H_e) = 8.4 Hz, ³J(P, H_e) = 51.6 Hz, CH₂), 3.57 (1H, q, ²J(H_a, H_e) = 8.4 Hz, ³J(P, H_a) = 41.3 Hz, CH₂), 7.49 (1H, d ¹J(P, H) = 772.5 Hz, PH); ³¹P{¹H} NMR (CD₂Cl₂) δ –49.21, 148.45 ppm; IR ν_{max}(nujol)/cm^{–1} 716vs, 924vs, 977vs, 1047s, 1160vs ν(C–O–P), 2362s ν(P–H), 3350s ν(N–H); ESI-MS: *m/z* calcd for [M + H]⁺ 236.14 found 236.14.

4.3. Synthesis of the complexes

4.3.1. [PdCl₂{P(OCMe₂CMe₂O)OCMe₂CMe₂NH₂}] **2**

[PdCl₂(cod)] (0.19 g, 0.67 mmol) was added to a solution of HP(OCMe₂CMe₂O)(OCH₂CMe₂NH) (0.24 g, 1.02 mmol) in dichloromethane (4 cm³). The yellow suspension was stirred for 20 min to produce a yellow solution. The crude product was precipitated with ethyl ether. The obtained precipitate was filtered, washed with ethyl ether and dried *in vacuo*. Yield: 0.25 g (91%) Single crystals suitable for X-ray analysis were obtained from acetone solution by slow evaporation.

Anal. Calc. for C₁₀H₂₂Cl₂NO₃PPd: C, 29.11; H, 5.37; N 3.39 Found: C, 29.84; H, 5.43; N, 3.38%; ¹H NMR (CD₂Cl₂) δ 1.34, 1.54, 1.58 (18H, s, s, CH₃), 3.93 (2H, br s, NH₂), 4.01 (2H, d, ³J(P, H) = 18.7 Hz, CH₂); ³¹P NMR (CD₂Cl₂) δ 90.70 ppm; IR ν_{max}(nujol)/cm^{–1} 279vs, 289vs ν(Pd–Cl), 916s, 958vs, 1031s, 1136s ν(C–O–P), 3126m, 3198m ν(N–H₂); ESI-MS: *m/z* calcd for [M + Na]⁺ 433.96 found 433.96.

4.3.2. [PdCl(C₃H₅){P(OCMe₂CMe₂O)OCMe₂CMe₂NH₂}] **3**

[Pd(μ-Cl)(C₃H₅)₂] (0.13 g, 0.35 mmol) was added to a solution of HP(OCMe₂CMe₂O)(OCH₂CMe₂NH) (0.21 g, 0.89 mmol) in toluene (4 cm³). The yellow solution was stirred for 30 min at room temperature, and during that time a white precipitate started to form in the system. The obtained product was filtered, washed with ethyl ether and dried *in vacuo*. Yield: 0.25 g (84%) Anal. Calc. for C₁₃H₂₇ClNO₃PPd: C, 37.34; H, 6.51; N 3.35 Found: C, 37.56; H, 6.55; N, 3.36%; ¹H NMR (CDCl₃) δ 1.26, 1.34, 1.42 (18H, s, s, CH₃), 3.12 (2H, br s, CH₂), 3.95 (4H, br d, CH₂), 5.01 (br s NH₂), 5.65 (1H, m, CH); ³¹P NMR (CDCl₃) δ 134.85 ppm; IR ν_{max}(nujol)/cm^{–1} 290vs ν(Pd–Cl), 460m, 469m, ν(Pd–C), 925vs, 951s, 1136m ν(C–O–P), 3163m, 3239m ν(N–H₂); ESI-MS: *m/z* calcd for [M – Cl]⁺ *m/z* 382.08; found 382.08.

4.4. Crystal structure determinations

The data were collected on a KM4CCD diffractometer and corrected for Lorentz and polarisation effects. Data reduction was carried out using the Oxford Diffraction (Poland) programs. The structures were solved by direct method using SHELXS and refined

by the full-matrix least-squares method on F^2 using the SHELXL software [23]. Non-hydrogen atoms were refined with anisotropic thermal parameters. The hydrogen atoms were set in calculated positions and refined using the riding model with a common fixed isotropic thermal parameter.

4.5. Representative Heck reaction procedure

The Heck reactions were carried out under a nitrogen atmosphere in a 50 cm³ Schlenk tube equipped with a magnetic stirrer. In a typical experiment, the flask was charged with the reagents: the catalyst (1.35×10^{-5} mol), bromobenzene PhBr 0.46 cm³ (4.36×10^{-3} mol) and *n*-butyl acrylate CH₂=CHC(O)OBu 0.27 cm³ (1.9×10^{-3} mol) in DMF as a solvent (3 cm³) containing mesitylene as an internal standard. [ⁿBu₄N]Br 0.75 g (2.3×10^{-3} mol) and the base NaHCO₃ 0.37 g (4.4×10^{-3} mol) were used as additives. The mixture was heated to 140 °C and stirred for 4 h. After that time, the reaction mixture was cooled and organic products were separated by extraction with diethyl ether (3 times with 7 cm³), washed with water, dried over MgSO₄ and analysed by GC–MS. The structures of the synthesised (*E*)-Stilbenes were confirmed by GC–MS and NMR spectroscopy, matching data reported in the literature [24].

4.6. Hiyama reaction procedure

The Hiyama reactions were carried out under a nitrogen atmosphere in a 50 cm³ Schlenk tube equipped with a magnetic stirrer. In a typical experiment, the flask was charged with the reagents: the catalyst (1.31×10^{-5} mol), bromobenzene PhBr 0.14 cm³ (1.31×10^{-3} mol), ArCH=CH[Si] 1.44 × 10⁻³ mol in DMF as a solvent (2 cm³) containing mesitylene as an internal standard. The activator [ⁿBu₄N]F (2.14×10^{-3} mol) was used as an additive. The mixture was heated to 140 °C and stirred for 4 h. After that time the reaction mixture was cooled and organic products were separated by extraction with diethyl ether (3 times with 7 cm³), washed with water, dried over MgSO₄, and analysed by GC–MS.

Acknowledgements

Financial support of the Polish Ministry of Science and Higher Education (Grant No N204 028538) is gratefully acknowledged. The authors are grateful to Dr Mariusz Majchrzak for preparing styrylsilanes and Ms Marzena Dejerling for testing the Heck and Hiyama reactions.

Appendix A. Supplementary material

CCDC 810570–810572 contain the supplementary crystallographic data for compound **1**, **2** and **4**, respectively. These data can be obtained free of charge from The Cambridge Crystallographic Data Centre via www.ccdc.cam.ac.uk/data_request/cif.

Appendix. Supplementary material

Supplementary data associated with this article can be found, in the online version, at doi:10.1016/j.jorganchem.2011.05.008.

References

- [1] (a) P.W.N.M. van Leeuwen, P.C.J. Kamer, C. Claver, O. Pámies, M. Diéguez, *Chem. Rev.* 111 (2011) 2077–2118; (b) A. Marson, J.E. Ernsting, M. Lutz, A.L. Spek, P.W.N.M. van Leeuwen, P.C.J. Kamer, *Dalton Trans.* (2009) 621–633; (c) Y. Mata, M. Diéguez, O. Pámies, C. Claver, *Org. Lett.* 7 (2005) 5597–5599; (d) K.N. Gavrilov, O.G. Bondarev, A.V. Korostylev, A.I. Polosukhin, V.N. Tsarev, N.E. Kadilnikov, S.E. Lyubimov, A.A. Shiryaev, S.V. Zheglov, H.-J. Gais, V.A. Davankov, *Chirality* 15 (2003) S97–S103; (e) K.N. Gavrilov, O.G. Bondarev, A.I. Polosukhin, *Russ. Chem. Rev.* 73 (2004) 671–699.
- [2] A. Skarżyńska, A.M. Trzeciak, M. Siczek, *Inorg. Chim. Acta* 365 (2011) 204–210.
- [3] A. Skarżyńska, A.M. Trzeciak, *Synthesis* submitted.
- [4] R. Burgada, R. Setton, F.R. Hartley (Eds.), *The Chemistry of Organophosphorus Compounds*, 3, Wiley Interscience, New York, 1993, p. 185.
- [5] B.A. Arbutov, N.A. Polezhaeva, *Russ. Chem. Rev.* 43 (1974) 933–973.
- [6] K.N. Gavrilov, A.I. Polosukhin, O.G. Bondarev, S.E. Lyubimov, K.A. Lyssenko, P.V. Petrovskii, V.A. Davankov, *J. Mol. Catal. A: Chem.* 196 (2003) 39–53.
- [7] R. Burgada, C. Laurencio, *J. Organomet. Chem.* 66 (1974) 255–270.
- [8] A.V. Korostylev, O.G. Bondarev, K.A. Lyssenko, A.Yu. Kovalevsky, P.V. Petrovskii, G.V. Tcherkaev, I.S. Mikhel, V.A. Davankov, K.N. Gavrilov, *Inorg. Chim. Acta* 295 (1999) 164–170.
- [9] V.F. Zheltukhin, A.I. Dovbysh, D.N. Sadkova, A.B. Dobrynin, O.N. Kataeva, I.A. Litvinov, V.A. Alfonsov, *Russ. Chem. Bull. Int. Ed.* 54 (2005) 1935–1938.
- [10] P.F. Meunier, R.O. Day, J.R. Devillers, R.R. Holmes, *Inorg. Chem.* 17 (1978) 3270–3276.
- [11] L. Yu, Z. Liu, H. Fang, Q.L. Zeng, Y.F. Zhao, *Amino Acids* 28 (2005) 369–372.
- [12] L. Yu, Z. Liu, H. Fang, Y.-F. Zhao, *Acta Crystallogr. E* 61 (2005) o261–o262.
- [13] N.D. Jones, S.Jo. Ling Foo, B.O. Patrick, B.R. James, *Inorg. Chem.* 43 (2004) 4056–4063.
- [14] K.N. Gavrilov, O.G. Bondarev, R.V. Lebedev, A.A. Shiryaev, S.E. Lyubimov, A.I. Polosukhin, G.V. Grintsev-Knyazev, K.A. Lyssenko, S.K. Moiseev, N.S. Ikonnikov, V.N. Kalinin, V.A. Davankov, A.V. Korostylev, H.-J. Gais, *Eur. J. Inorg. Chem.* (2002) 1367–1376.
- [15] A.V. Korostylev, O.G. Bondarev, S.Y. Lyubimov, A.Yu. Kovalevsky, P.V. Petrovskii, V.A. Davankov, K.N. Gavrilov, *Inorg. Chim. Acta* 303 (2000) 1–6.
- [16] (a) M. Diéguez, O. Pámies, Y. Mata, E. Teuma, M. Gómez, F. Ribaudó, P.W.N.M. van Leeuwen, *Adv. Synth. Catal.* 350 (2008) 2583–2598; (b) N.T.S. Phan, M. Van Der Sluys, C.W. Jones, *Adv. Synth. Catal.* 348 (2006) 609–679; (c) J.A. Widgren, R.G. Finke, *J. Mol. Catal. A: Chem.* 198 (2003) 317–341; (d) J. Li, M. Lutz, A.L. Spek, G.P.M. van Klink, G. van Koten, R.J.M. Klein Gebbink, *J. Organomet. Chem.* 695 (2010) 2618–2628.
- [17] (a) G.M. Whitesides, M. Hackett, R.L. Brainard, J.-P.P.M. Lavalleye, A.F. Sowinski, A.N. Izumi, S.S. Moore, D.W. Brown, E.M. Staudt, *Organometallics* 4 (1985) 1819–1830; (b) F. Fernández, B. Cordero, J. Durand, G. Muller, F. Malbosc, Y. Kihn, E. Teuma, M. Gómez, *Dalton Trans.* (2007) 5572–5581.
- [18] C.C. Cassol, A.P. Umpierre, G. Machado, S.I. Wolke, J. Dupont, *J. Am. Chem. Soc.* 127 (2005) 3298–3299.
- [19] D.D. Perrin, W.L.F. Armarego, *Purification of Laboratory Chemicals*, third ed. Pergamon Press, Oxford, 1998.
- [20] D. Drew, J.R. Doyle, *Inorg. Synth.* 13 (1972) 52.
- [21] Y. Tatsuno, T. Yoshida, S. Otsuka, *Inorg. Synth.* 28 (1990) 342–345.
- [22] D. Houalla, M. Sanchez, L. Beslier, R. Wolf, *Org. Magn. Reson.* 3 (1971) 45–74.
- [23] G.M. Sheldrick, *Acta Crystallogr. A* 64 (2008) 112–122.
- [24] (a) Y. Leng, F. Yang, K. Wei, Y. Wu, *Tetrahedron* 66 (2010) 1244–1248; (b) R. Cella, A. Stefani, *Tetrahedron* 62 (2006) 5656–5662 and references therein.